Biogeosciences

Open Access

Supplement of

Technical note: Rapid image-based field methods improve the quantification of termite mound structures and greenhouse-gas fluxes

Philipp A. Nauer et al.

Correspondence to: Philipp A. Nauer (pnauer@unimelb.edu.au)

1 Additional details on the image-based methods to quantify termite mound structures

1.1 Photogrammetry method

To generate a complete representation of the termite mound (TM), 40-50 photographs covering two to three panoramas were acquired at different heights: close to the soil surface at ~0.5, at breast-height ~1-1.5, and on top of the TM ~1.5-2.5 m above ground (Fig. S1a). Images were shot in steps of approximately 22.5 ° and at 1-2 m distance around the TM. The focal distance was manually fixed for each panorama and ranged between 14-25 mm, depending on the size of the TM and the surroundings. The digital reconstruction workflow in Agisoft Photoscan™ consisted of three steps: generation of a sparse point cloud (tie points) via SfM algorithms (Fig. S1a), dense multi-view stereo (MVS) matching to generate a dense point cloud (Fig. S1b), and construction of a 3D triangular mesh with texture based on the dense point cloud (Fig. S1c; Agisoft LLC, 2017; Szeliski, 2010). The mesh was scaled in the software package Meshlab (Cignoni et al., 2008), by determining the dimensions of the reconstructed reference object ten times, then calculating the mean and applying a uniform scaling factor based on the known dimensions of the object. All non-TM parts of the mesh (outside of and including the pink marker paint) were deleted to create an "open" mesh consisting of the epigeal TM open at its base. After calculating the surface area of the mesh, it was closed with the "Fill Hole" algorithm in Meshlab (Liepa, 2003), to calculate the epigeal volume and basal area of the TM.
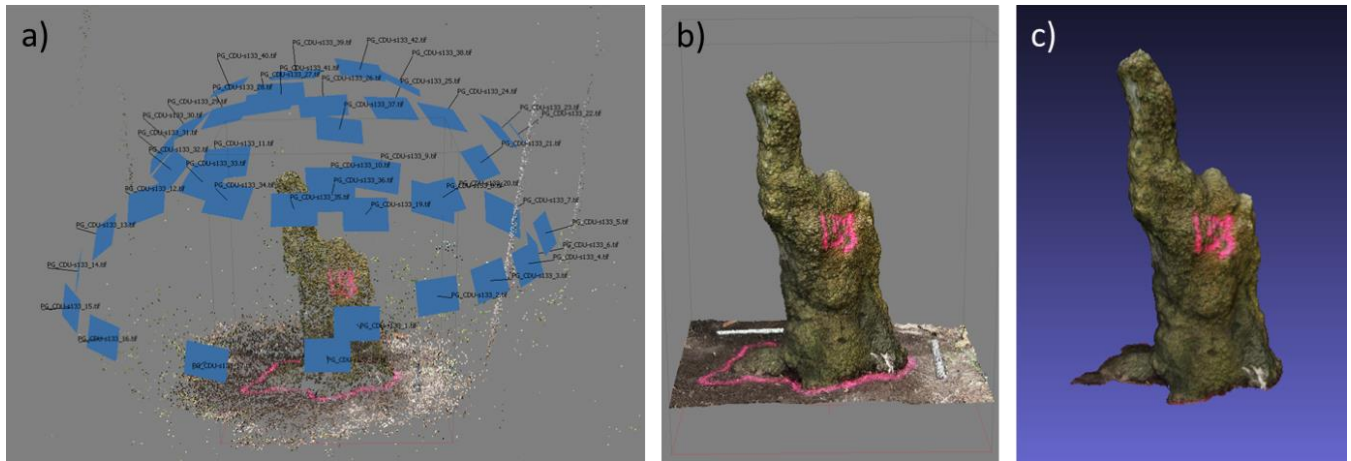

Fig. S1: Illustration of the PG processing steps. (a) reconstruction of camera positions and sparse point cloud; (b) generation of a dense point cloud and subsequent triangular mesh; (c) removal of reference objects and surrounding soil, and calculation of geometric measures of the scaled TM. Steps (a) and (b) were performed in Agisoft Photoscan™, and step (c) in Meshlab.
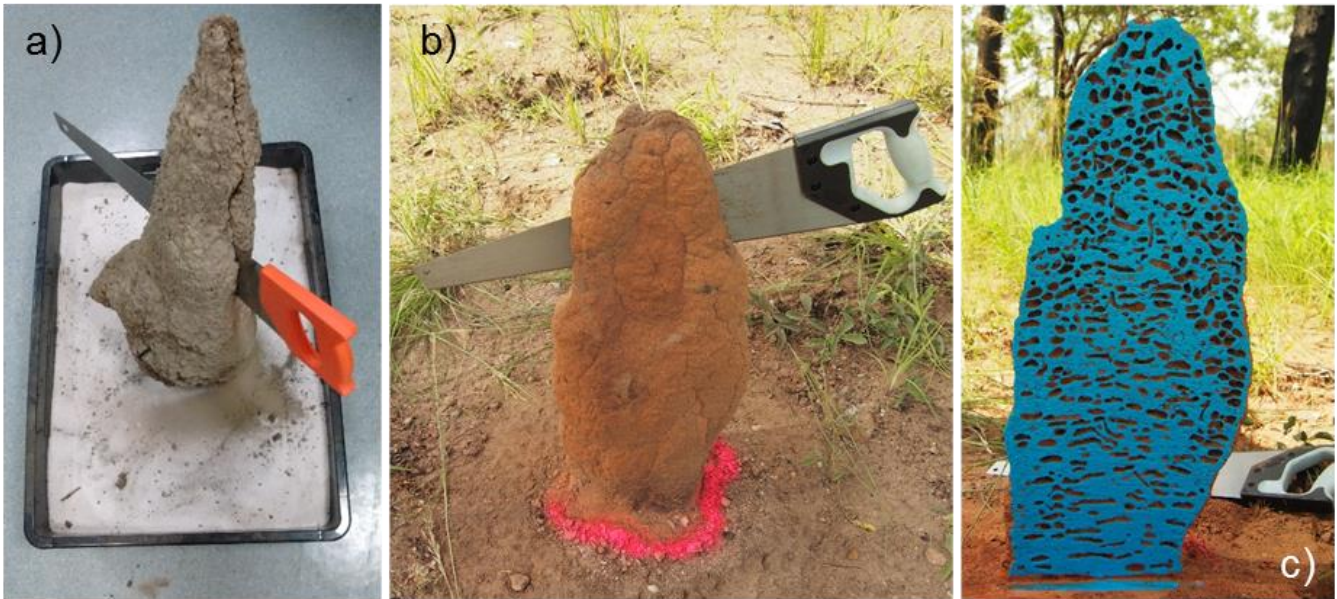
1.2 Cross-sectioning method

Fig. 2: Cross sectioning of TMs with a wood saw; (a) in the laboratory with excavated TMs placed in a sand box; and (b,c) an exemplary application in the field by cutting the epigeal part vertically and at its base, then painting the remaining half.

5   The cross-sectioning method was applied in the laboratory with fully excavated TMs placed in a sand box (Fig. S2a). However, it is possible to apply the method directly in the field on epigeal TMs (Fig. S2b,c). For sectioning the TMs, low-cost hand saws designed for wood were used, but needed to be replaced relatively frequently when becoming blunt. For painting we used a common firm paint roller and viscous water-based paint (Aquanamel, DULUX Group Ltd, Clayton, Australia) of bright blue colour ("Tall Ships") that we diluted only slightly to avoid painting parts of the cavities. The paint

10   had its hue maximum between 140-150 in the HSB colour space. The colour image (Fig. S3a) was converted to binary (Fig. S3b) with a colour threshold of $\pm$ 25 hue values around the hue maximum using the software package Fiji (Schindelin et al., 2012). The binary image was segmented with the active contour algorithm implemented in the Level Sets plugin (Yoo, 2004), and subsequently filled using Fiji's built-in function "Fill holes" (Fig. S3b).
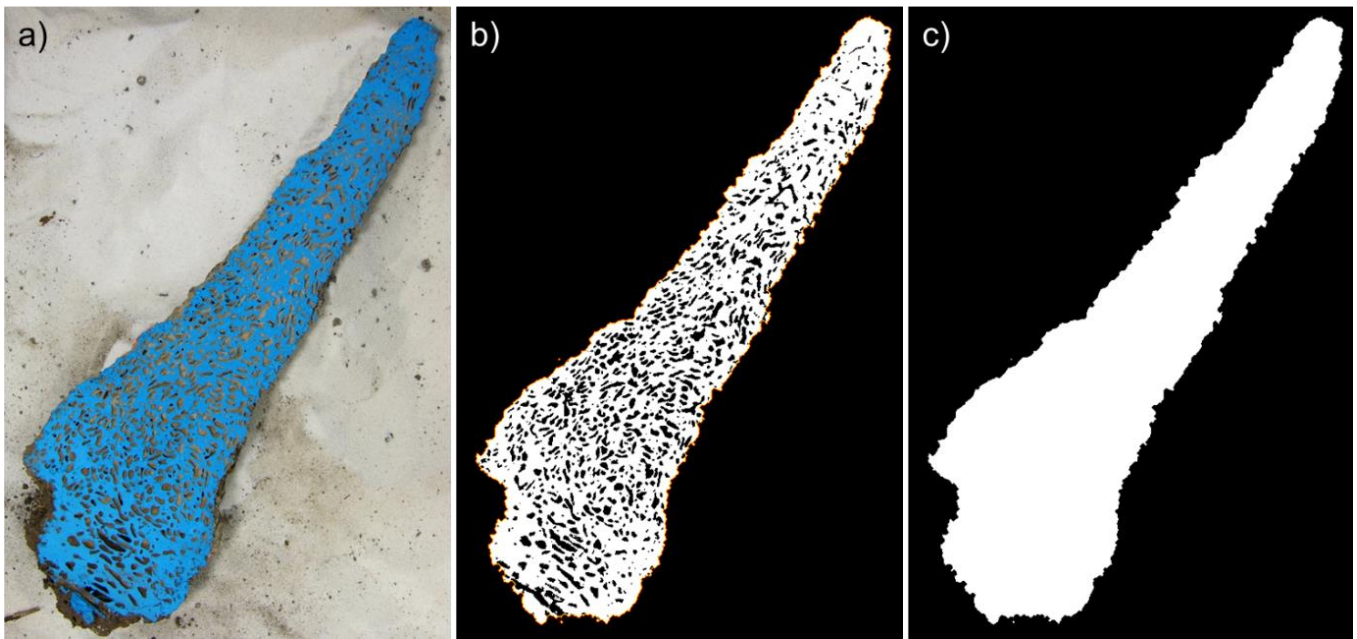
Fig. S3: Painted cross section colour image (a) and corresponding open (b) and filled (c) binary images of mound Mn6. The thin red line around the open TM is the result of segmentation using an active contour algorithm and represents the outer boundary of the TM.

1.3 X-ray tomography (CT scanning) method

Termite mounds were scanned with a Philips Ingenuity medical CT scanner with exposure parameters of 120 kV and 400 mAs. Tomographic scans were reconstructed into a 768x768 pixel matrix with a constant slice thickness of 1.5 mm and 0.75 mm interslice distance, resulting in a partial overlap of slices. The number of slices varied with the size of the mounds, as well as the effective size of the pixels, ranging between 0.36-0.65 mm. Original DICOM images were imported into the Fiji software package, converted to 8-bit grayscale PNG files (Fig. S4a), then converted to binary using the "Default" thresholding method in the Auto Threshold plugin of Fiji (Fig. S4b), which is based on the isodata algorithm (Ridler and Calvard, 1978). Preliminary analysis showed that this method consistently performed best in differentiating the TM walls (including incorporated roots and pieces of wood) from the chambers for all termite species. Water did not influence the CT scans of TMs, as it is present only in micro-pores and thus not visible due to the limited resolution of the medical-grade scanner used. Holes of the binary images were filled with the same algorithms used in the cross-sectioning method.
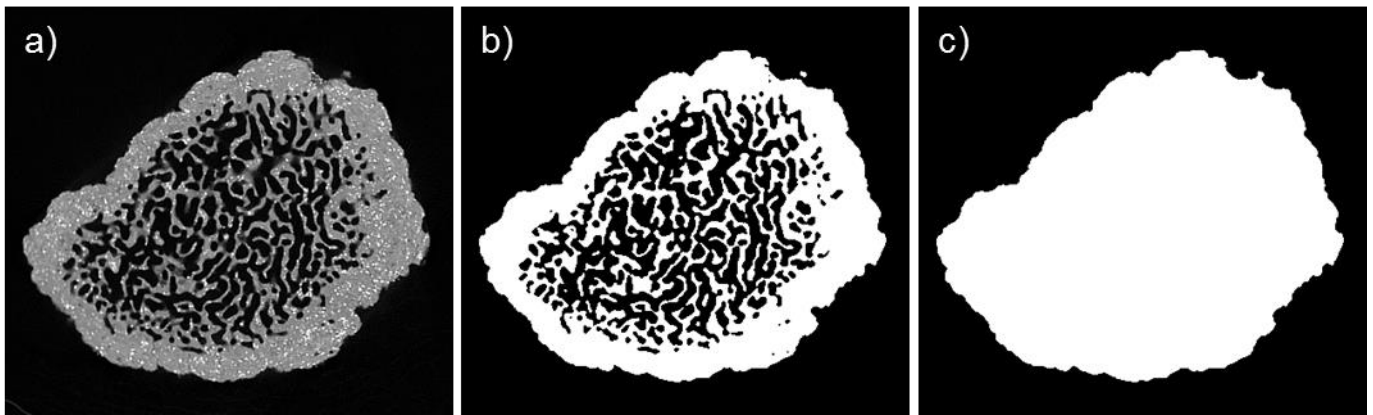
Fig. S4: Individual slice of the CT scan of mound Tp1 (a) and corresponding open (b) and filled (c) binary images.

References

Agisoft LLC: Agisoft PhotoScan User Manual - Standard Edition, Version 1.3, 2017.

5 Cignoni, P., Callieri, M., Corsini, M., Dellepiane, M., Ganovelli, F. and Ranzuglia, G.: MeshLab: an Open-Source Mesh Processing Tool, in Sixth Eurographics Italian Chapter Conference, pp. 129–136., 2008.

Liepa, P.: Filling holes in meshes, in Proceedings of the 2003 Eurographics/ACM SIGGRAPH symposium on Geometry processing, pp. 200–205, Eurographics Association, Aire-la-Ville, Switzerland., 2003.

Ridler, T. and Calvard, S.: Picture Thresholding Using an Iterative Selection Method, IEEE Trans. Syst. Man. Cybern., 8(8),

10 630–632, doi:10.1109/TSMC.1978.4310039, 1978.

Schindelin, J., Arganda-Carreras, I., Frise, E., Kaynig, V., Longair, M., Pietzsch, T., Preibisch, S., Rueden, C., Saalfeld, S. and Schmid, B.: Fiji: an open-source platform for biological-image analysis, Nat. Methods, 9(7), 676–682, 2012.

Szeliski, R.: Computer Vision : Algorithms and Applications - Chapter 3 Image processing, Comput. Vis. Algorithms Appl., 110, doi:10.1007/978-1-84882-935-0, 2010.

15 Yoo, T. S.: Insight into Images: Principles and Practice for Segmentation, Registration, and Image Analysis, AK Peters Ltd., 2004.

Table S1: Geometric measures of the 29 investigated termite mounds of the three termite species *Microcerotermes nervosus* (Mn), *Macrognathotermes sunteri* (Ms) and *Tumulitermes pastinator* (Tp). Abbreviations of TM parameters: height (h); basal radius (r_B); epigeal volume (V_E); epigeal surface area (A_E); basal area (A_B).

	Field measurement		Photogrammetry		
	h	r_B	V_E	A_E	A_B
Termite mound	(m)	(m)	(L)	(m^2)	(m^2)
Mn1 [a,b,c]	0.36	0.10	4.58	0.17	0.052
Mn2 [a,b,c]	0.59	0.11	6.34	0.22	0.037
Mn3 [c]	0.35	0.13	6.80	0.19	0.070
Mn4 [a,b,c]	0.39	0.13	7.19	0.21	0.045
Mn5	0.84	0.12	10.7	0.34	0.047
Mn6 [a,b,c]	0.71	0.15	11.4	0.30	0.077
Mn7	0.78	0.14	11.5	0.33	0.058
Mn8 [a,b,c]	0.62	0.14	13.2	0.35	0.084
Mn9 [a,b,c]	0.67	0.16	14.0	0.35	0.084
Mn10	0.79	0.15	18.2	0.41	0.081
Ms1 [a,b,c]	0.37	0.08	5.21	0.18	0.028
Ms2 [c]	0.56	0.09	6.80	0.22	0.14
Ms3 [a,b,c]	0.35	0.11	7.16	0.24	0.094
Ms4 [c]	0.18	0.19	8.19	0.20	0.12
Ms5 [a,b,c]	0.48	0.18	13.3	0.42	0.21
Ms6 [a,b,c]	0.47	0.21	19.1	0.39	0.15
Ms7 [a,b,c]	0.60	0.16	28.4	0.53	0.10
Ms8	0.73	0.34	95.8	1.70	1.1
Ms9	1.30	0.33	99.5	1.5	0.38
Ms10	1.0	0.50	192	2.2	0.66
Tp1 [a,b,c]	0.18	0.16	6.60	0.18	0.073
Tp2 [a,b,c]	0.22	0.17	8.59	0.19	0.093
Tp3 [a,b,c]	0.28	0.18	12.2	0.28	0.15
Tp4 [a,b,c]	0.41	0.15	16.4	0.35	0.074
Tp5 [a,b,c]	0.37	0.17	16.9	0.33	0.10
Tp6 [a,b,c]	0.50	0.18	24.8	0.45	0.12
Tp7	0.86	0.45	169	1.5	0.69
Tp8	1.0	0.45	250	2.3	0.57
Tp9	0.84	0.47	266	2.2	0.76

[a] scanned with CT; [b] cross-sectioned; [c] CH$_4$ flux measured

5